ISSN 2278-8808
An International Peer Reviewed
SCHOLARLY RESEARCH JOURNAL
FOR INTERDISCIPLINARY STUDIES

ELECTROCHEMICAL INHIBITION STUDIES ON STEEL IN ACIDIC MEDIUM

Surendra Singh, Ph. D.

M.Sc., M.Phil., Ph.D., Associate Professor, Dept of Chemistry, Govt. Degree College, Mant, Mathura (U.P.)

Abstract

As Anise oil (AO) is taken into account a green inhibitor of steel (CS) corrosion, the electrochemical behavior of CS was examined by electrochemical impedance spectroscopy (EIS) and potentiodynamic polarization to calculate its corrosion resistance in 0.5 M acid containing different concentrations of AO before and after irradiation with γ-rays (5 kGy and 15 kGy). Potentiodynamic polarization proved that the best value of inhibition efficiency is 95.3% obtained by 50 ppm AO after irradiation with γ-rays at 298 K. The EIS results indicate that the changes in impedance parameters are associated with the adsorption of AO and its coverage of the CS surface. A scanning microscope (SEM) was accustomed distinguish between the corroded surface and therefore the unharmed surface thanks to the irradiated AO inhibitor. All this results emphasize the facility of using AO as a green inhibitor with γ-rays that may protect the CS surface, which is able to extend its industrial applications with high efficiency.

Keywords: *Potentiodynamic polarization; carbon steel; anise oil; gamma irradiation; EIS; FT-IR; SEM*

Introduction

Carbon steel (CS) is widely utilized in marine applications, chemical processing, petroleum production and refining, construction and metal-processing equipment. they need been found to be very useful and economical [1,2] despite its high corrosion susceptibility. These applications usually induce a heavy corrosive effect on equipment, tubes, and pipelines made from iron and its alloys [3]. The investigation of corrosion of iron and its alloys may be a subject of enormous experimental preoccupation because of the economic losses and environmental pollution caused by this phenomenon during the manufacture of metal alloys [4,5].

The use of chemical inhibitors is a vital method of protecting metallic materials against dissolution because of the corrosion phenomenon. However, toxicity and therefore the high cost of chemical compounds led researchers to seem for other alternatives like using green

inhibitors extracted from various plants [10]. The green or eco-friendly inhibitors exhibited excellent efficiency as corrosion inhibitors for various metals and alloys in acidic media [11,12]. Some tested the effect of oil compounds, while others studied the employment of extract compounds [16,17].

To the most effective of our knowledge, little research is reported in literature about using irradiation of Anise oil (AO) with various doses of γ-rays (5 kGy and 15 kGy) as a corrosion inhibitor for CS in acid medium. This research work aims to check the effect of AO as a green economic inhibitor before and after various doses of γ-rays on the inhibition of the corrosion rate of CS in 0.5 M acid solution. During this respect, potentiodynamic polarization and electrochemical impedance spectroscopy (EIS) methods were accustomed evaluate the electrochemical behavior of CS in an acid medium. The surface morphology was studied by scanning microscopy (SEM) under different studying conditions.

Materials and methods

Samples and solutions

Samples **within the** present study were composed of a CS rod with a cross-sectional area of 1 cm2 and its chemical composition was analyzed by X-ray fluorescence as shown in Table 1. These samples act as a working electrode (WE). All the chemicals were analytical grade Aldrich products. **Acid** solution with 0.5 M and triple **water** were **utilized in** all the investigations. Before performing the experiments, the working electrode was abraded with **abradant of various** grades up to 1,200 grit, then rubbed with a smooth polishing cloth, washed with triple **water**, and transferred to the three-electrode electrochemical cell.

Table 1: Chemical composition (wt%) of the investigated CS sample.

C	Mn	S	P	Fe
0.22	0.9	0.03	0.03	Balance

Table 1: Chemical composition (wt%) of the investigated CS sample.

Inhibitor

AO (trans-p-propenylanisole (anethole), trans-1-methoxy-4-(1-propenyl)benzene) with molar mass 148.2 g/mol and **chemical formula** C10H12O was **employed in** an analytical grade from El-Captain Company (CAP PHARM). AO, obtained from star anise native to China or **anise** native to the Mediterranean region, is an aromatic **yellowness** oily liquid composed mainly of anethole (propenylanisole). The star anise is unrelated botanically to the anise of

the Bible but **includes a** very similar taste and aroma. **It's utilized in** medicinal cough drops, dentifrices, perfumes, flavorings, beverages, candies, and embedding materials for microscopy [21]. AO was irradiated by various doses of γ-rays (i.e., 5 kGy and 15 kGy, resp.) before **getting used** as an inhibitor. So, AO **will be** considered as an environmentally safe and economically reasonable green inhibitor.

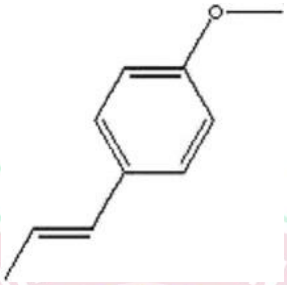

Figure 1: Trans-1-methoxy-4-(1-propenyl)benzene, transp-propenylanisole.

All the electrochemical measurements, including potentiodynamic and electrochemical impedance spectroscopy (EIS), were conducted using Gamry PCI300/4.

Potentiostat/Galvanostat/Zra analyzer. EIS **may be a** nondestructive sensitive technique **that permits** the detection of any changes occurring at the electrode/electrolyte interface. Impedance data were presented as Nyquist plots. The impedance measurements were **administered** at the **electric circuit** potential (OCP) **in a very** frequency range from 0.01 Hz up to 100 kHz with a superimposed AC-signal amplitude of 5 mV peak to peak. EIS can measure directly the impedance, Z, **and also the** phase shift of the electrochemical system. All electrochemical tests were **distributed employing a** three-electrode cell composed of **steel**, with an exposed **expanse** of 1 cm2, used as a working electrode, platinum **because the** counter electrode, and saturated calomel electrode (SCE) (ESCE = 0.242 V vs. **the traditional** hydrogen electrode (NHE)) as a reference electrode, respectively. Potentiodynamic measurements were **administered** at a scan rate of 3 mV/s at 25 °C. The Echem Analyst 5.21 statistically fits the experimental data to the Stern-Geary model for a corroding system. The routine automatically selects **the information** that lies within the Tafel region (±250 mV with **relevance** the corrosion potential). The Echem Analyst calculated the corrosion potential, the corrosion current density, **and also the** anodic and cathodic slopes,

$$IE\% = \frac{I_{corr} - I_{corr(inh)}}{I_{corr}} x100, \quad (1)$$

where Icorr and Icorr(inh) represent the corrosion current density values without and with inhibitor, respectively. Before impedance or polarization measurements, the working electrodes were immersed within the test solution until a gentle state of the OCP was reached. Each experiment was performed a minimum of twice with a replacement surface for every run.

Examination of surface morphology

A JEOL (5400 Japan) SEM was utilized to look at the surface morphology of varied specimens of CS after being immersed in 0.5 M acid within the absence and presence of the inhibitor at 50 ppm for 1 h. This instrument was operated during a secondary electron imaging mode with an accelerating voltage of either 10 KeV or 20 KeV. Within the present investigation, the magnification was selected, 100×. All the experiments were dole out at temperature 298 K unless otherwise stated. The experimental details are described in Section 3 [22].

2.5. Functional groups detection

The functional groups of AO were proved by infrared spectroscopy (FTIR). Inspection of Figure 2 shows that the characteristic band appeared at 519 cm−1 for stretching vibration of the aliphatic straight-chain −C−C− skeleton; the band**s appeared at 1,135 cm−1 and three, 217 cm−1 for stretching vibration of −CH(OH)− group.**

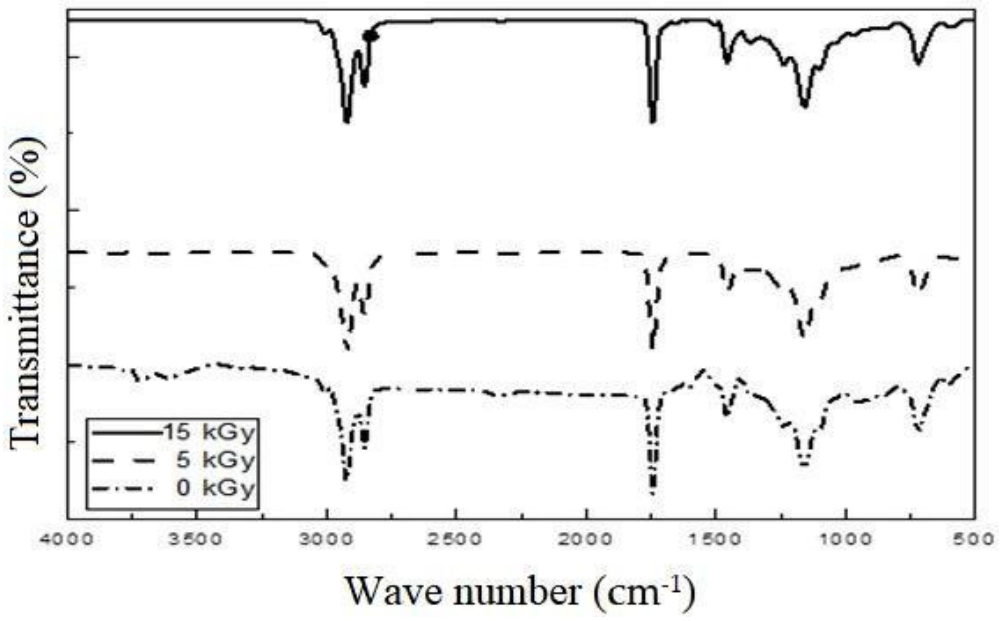

Figure 2: FTIR spectra of AO irradiated with various doses of γ-rays.

Results and discussion

OCP measurements

Figure 3 illustrates the potential-time curves of CS electrode in 0.5 M HCl solution against saturated calomel electrode (SCE): the blank curve was tending towards more negative value firstly, which represents the breakdown of the preimmersion, air formed oxide film present on the surface of working electrode. This oxide film was breakdown and soluble within the solution so the potential was shifted to a more negative direction until a steady-state potential was established at 500 V. Additions of the inhibitor molecules produce a negative shift Ecorr potential; these results indicated that the corrosion inhibitor may act as cathodic protection before and after being radiated.

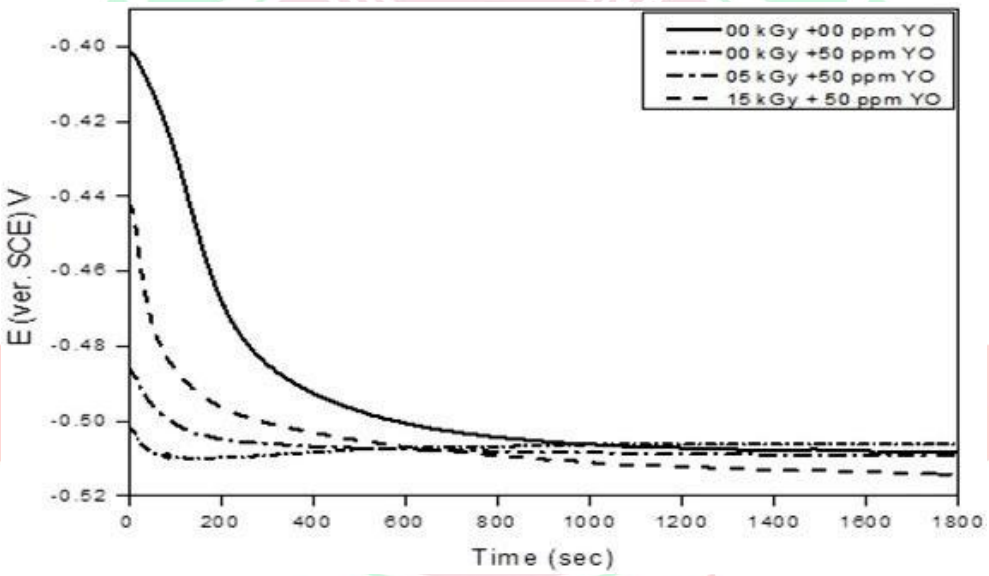

Figure 3: Potential-time curves for CS in 0.5 M HCl in the absence and presence of 50 ppm concentrations of the AO inhibitor before and after being radiated.

EIS measurements

The impedance results for the **chrome steel** in physiological solution after the immersion **for 2** different times are shown in Figures 4–6. EIS spectra illustrated typical Nyquist impedance plots obtained for the CS electrode at an OCP. **The simplest** fit using the equivalent circuit shown in Figure 7 and Table 2 illustrated that **the info** of this equivalent circuit showing the increasing inhibitor concentrations raised the polarization resistance (Rp). It also has been reported that the semicircles at high frequencies were generally **related to the comfort** of electrical double-layer capacitors, **and also the** diameters of the high-frequency capacitive

loops **are often** considered **because the** charge-transfer resistance. Table 2 illustrates the inhibition efficiency, η%, of AO inhibitor, being or without being radiated, for the CS electrode; and **it had been** calculated by **the subsequent** equation:

$$\eta\% = (R_p - R_{p0})/R_p x100, \quad (2)$$

where R_{p0} and R_p were the charge transfer resistance in absence and presence of AO inhibitor, respectively.

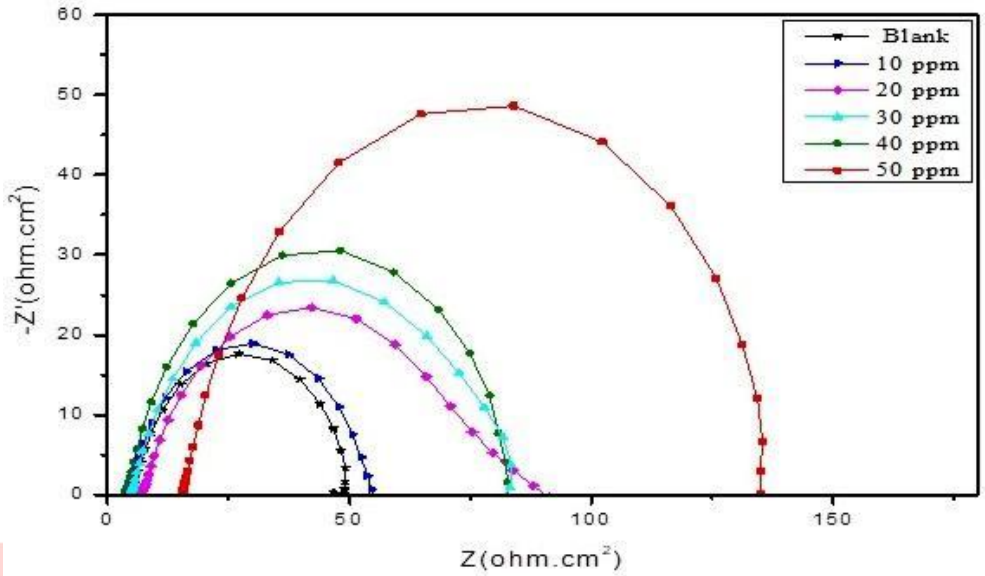

Figure 4: Nyquist for the corrosion of CS in 0.5 M HCl in the absence and presence of different concentrations of AO inhibitor at 25 °C.

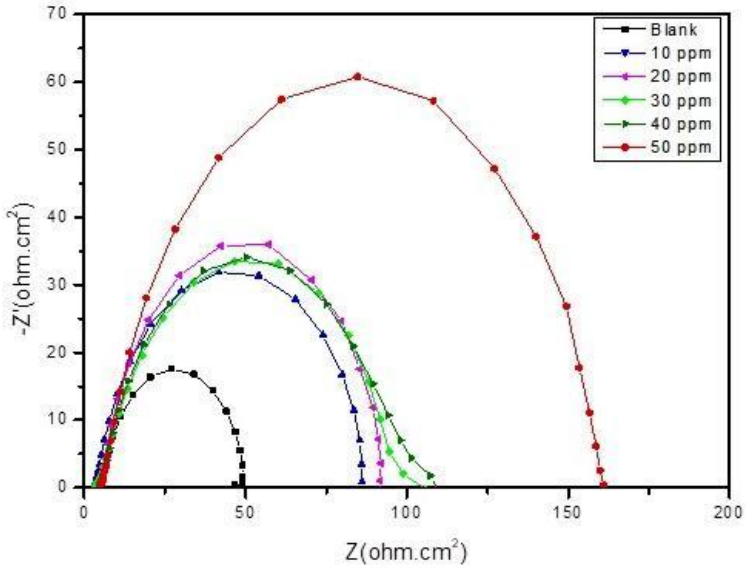

Figure 5: Nyquist for the corrosion of CS in 0.5 M HCl in the absence and presence of different concentrations of radiated AO inhibitor at 5 kGy.

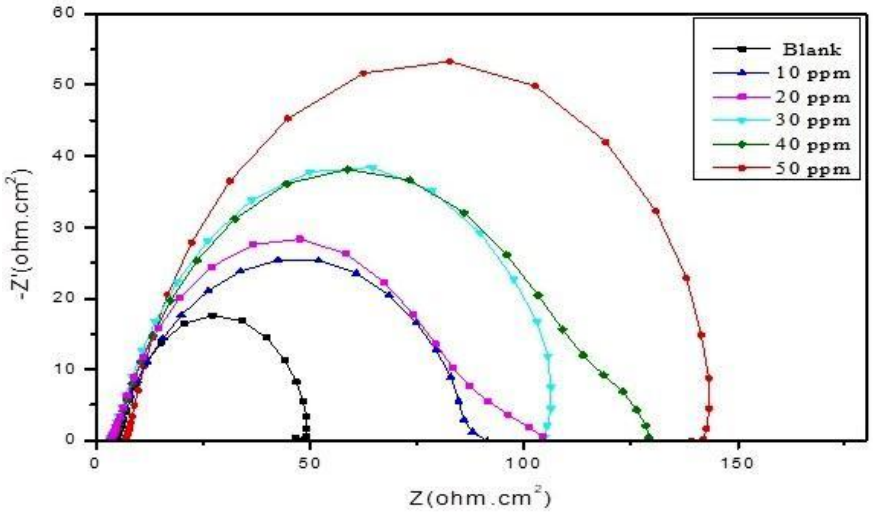

Figure 6: Nyquist for the corrosion of CS in 0.5 M HCl in the absence and presence of different concentrations of irradiated AO inhibitor at 15 kGy.

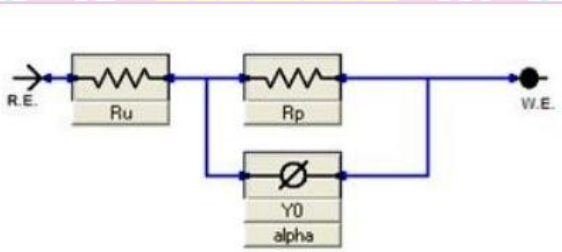

Figure 7: Equivalent circuit diagram used to fit the impedance data.

Table 2: Impedance parameters for the corrosion of CS in 0.5 M HCl without and with various concentrations of AO at 298 K.

Electrode	Inh. Conc.	Alpha	Y0 (S*s^a)	R_p (ohms)	R_u (ohms)	η (%)
CS	Blank	7.87E−01	0.003734	46	4.61E+00	0
	50 ppm	8.47E+02	0.009148	140	1.56E+01	67
	50 ppm + 5 kGy	7.98E+02	0.009525	161	5.02E+00	71
	50 ppm + 15 kGy	6.86E+02	0.009857	148	3.51E+00	69

Table 2: Impedance parameters for the corrosion of CS in 0.5 M HCl without and with various concentrations of AO at 298 K.

Electrochemical polarization measurements

The potentiodynamic polarization technique was **wont to** investigate the electrochemical behavior of CS in 0.5 M HCl solution. Representative polarization curves from the potentiodynamic polarization measurements are displayed in Figures 8–10. The quantitative corrosion parameters of corrosion potential (Ecorr), and corrosion current density (Icorr) obtained through the polarization curves were calculated and presented in Table 3. However, the differences in values of the inhibitors from those of the free acid solution **weren't** up to

85 mV; hence **they're** not sufficient to categorize the inhibitor as either of cathodic or anodic type. Therefore, AO **will be** considered as a mixed type inhibitor which inhibits the corrosion process by geometric blocking of both cathodic and anodic surface active sites of the CS. Also, corrosion current density was reduced **within the** presence of the inhibitors and with increasing the AO concentration, demonstrating the inhibitive effects of AO. The inhibition efficiency also increased with **the rise** in inhibitor concentration, **almost like** EIS. Figures 8–10 illustrate the potentiodynamic polarization curves for CS in 0.5 M HCl solution and **within the** presence of 50 ppm of the AO radiated and without being radiated. The electrochemical parameters, namely, corrosion potential (Ecorr), cathodic (bc) and anodic (ba) Tafel slopes, corrosion current density (Icorr) and inhibition efficiency (η%), **got** in Table 3.

T**he info** in Table 3 showed that the Icorr values decreased considerably with **the rise** of the inhibitor concentration, Ecorr were shifted to more negative values; therefore these inhibitors acted predominantly as cathodic inhibitors and consequently adsorption mechanism was **far more** likely at the cathodic sites. The effect of inhibitor type and concentration was observed on the values of ba and bc, **in order that** these inhibitors obstruct the available surface area; it seems that the film formed on the metallic surface became more uniform with concentration, while molecular structure may affect film resistance **thanks to** chemical bonding nature with metallic surface. The inhibition efficiency, η (%), was calculated and **it had been** obvious that the η (%) increased with increasing the inhibitor concentration. The mechanisms of the inhibiting effect **of those** derivatives were attributed to the formation of a chemical bonding between inhibitor and metallic surface **consistent with** oxygen-atoms. Adsorption of AO compound through oxygen molecules result from its capability of shearing lone pair electrons. **It's** noteworthy that the results obtained from potentiodynamic measurements matched with those obtained from Nyquist impedance determinations.

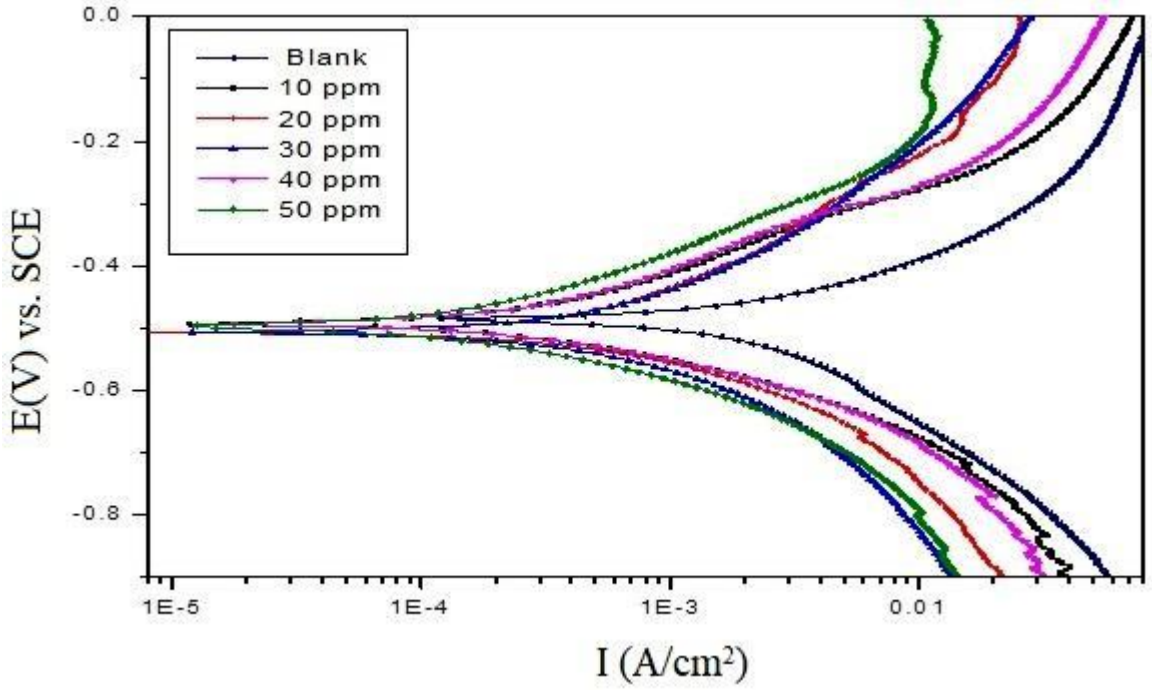

Figure 8: Potentiodynamic polarization plot for the corrosion of CS in 0.5 M HCl in the absence and presence of different concentrations of AO inhibitor at 25 °C.

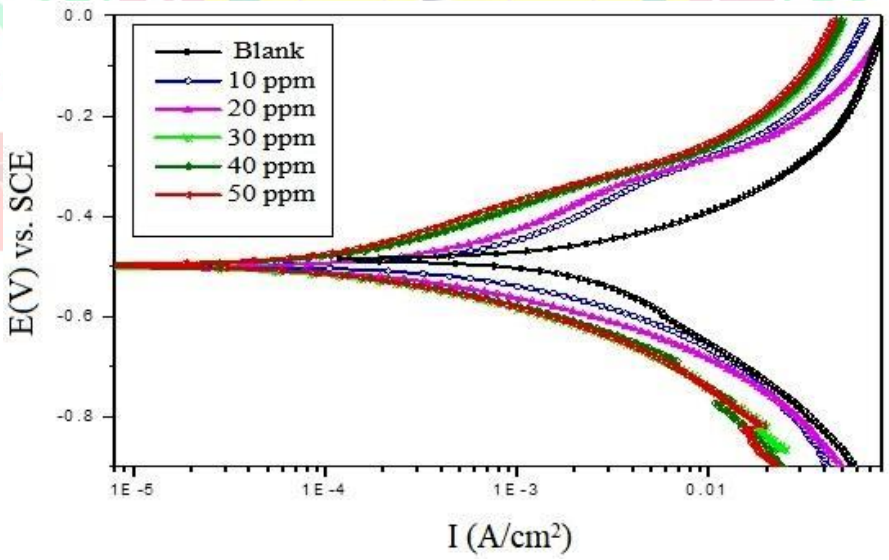

Figure 9: Potentiodynamic polarization plot for the corrosion of CS in 0.5 M HCl in the absence and presence of different concentrations of radiated AO inhibitor at 5 kGy at 25 °C.

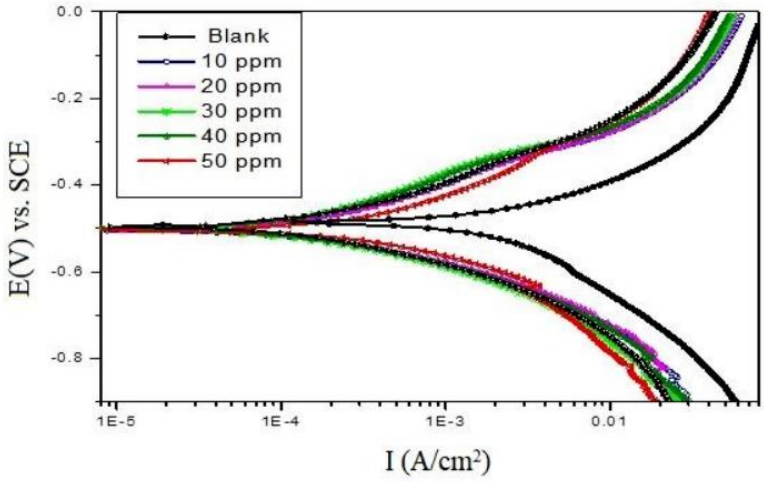

Figure 10: Potentiodynamic polarization plot for the corrosion of CS in 0.5 M HCl in the absence and presence of different concentrations of radiated AO inhibitor at 15 kGy at 25 °C.

Table 3: Polarization data of CS in 0.5 M HCl without and with various concentrations of AO at 298 K.

Electrode	Inh. Conc.	Ecorr. (mV)	Icorr. (μA/cm^2)	Tafel slopes		Corrosion rate (CR) (mpy)	η (%)
				β_a (V/decade)	β_c (V/decade)		
CS	Blank	−499	4,000	0.225	0.198	550	0
	50 ppm	−497	228	0.178	0.153	118	94
	50 ppm + 5 kGy	−505	210	0.147	0.114	108	95
	50 ppm + 15 kGy	−506	201	0.147	0.151	104	95

Table 3: Polarization data of CS in 0.5 M HCl without and with various concentrations of AO at 298 K.

Surface morphology

Scanning **microscopy** was **wont to** examine the surface morphology of the CS specimens immersed in 0.5 M HCl solution **within the** absence and presence of 50 ppm of AO inhibitor and also before immersion in acid medium and inhibitor. Figure 11(a) shows a characteristic surface of CS after polishing. Figure 11(b) shows the immersion of CS without AO inhibitor in 0.5 M HCl for 2 h. Scanning electron micrographs reveal that the surface was strongly damaged by corrosion (i.e., corroded surface), which is shown as black and white area on the surface of specimen. On **the opposite** hand, Figure 11(c) shows the surface of CS specimen after immersion in 0.5 M HCl and 50 ppm for 2 h. Scanning electron micrographs reveal that the surface was much less damaged. Figures 11(d) and 11(e) show that the formation of protective film of the inhibitor on the metal surface under the effect of gamma rays. The

results were obtained from the (SEM) technique explain those obtained from all electro chemical data.

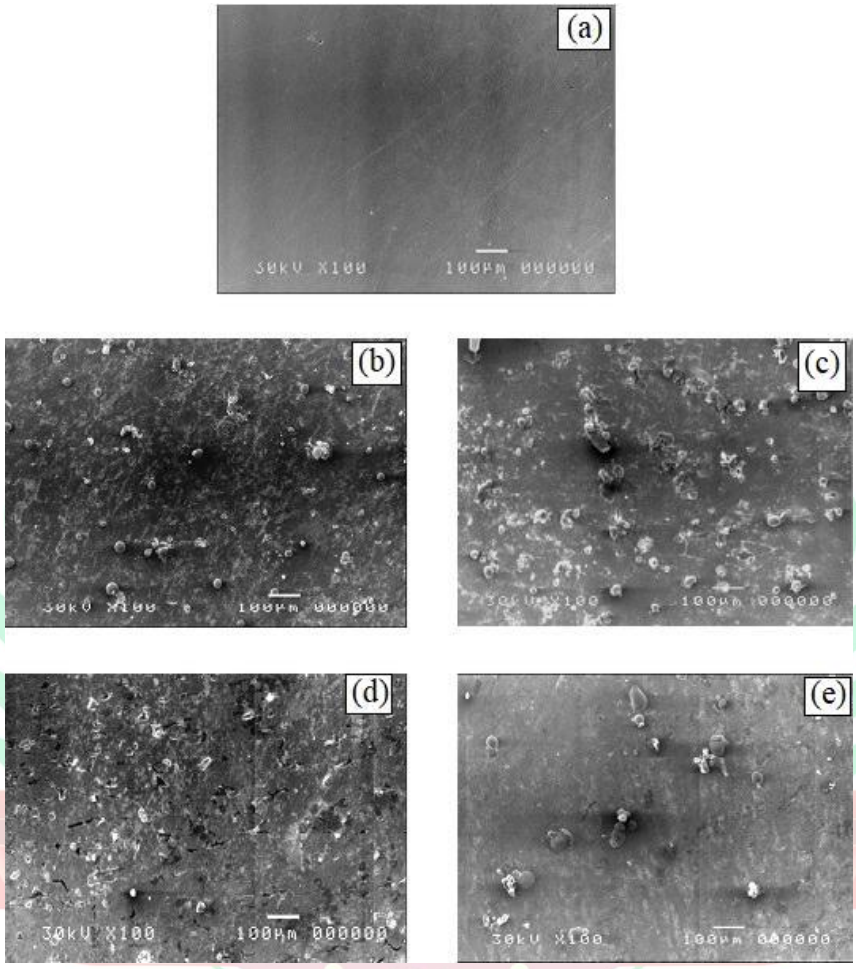

Figure 11: Scanning electron micrographs of CS: (a) CS after polishing; (b) CS immersion in 0.5 M HCl; (c) CS immersion in 0.5 M HCl + 50 ppm of inhibitor; (d) CS immersion in 0.5 M HCl + 50 ppm radiated inhibitor at 5 kGy; (e) CS immersion in 0.5 M HCl + 50 ppm radiated inhibitor at 15 kGy.

Conclusions

AO as a friendly corrosion inhibitor was examined for the primary time during this study at concentrations 0.0 ppm, 10 ppm, 20 ppm, 30 ppm, 40 ppm, and 50 ppm in 0.5 M HCl as electrolyte solution with two doses of nonparticulate radiation at 5 kGy and 15 kGy. The evaluation of the AO as an inhibitor was allotted by using electrochemical investigation. The online results indicated the superb effect of inhibitor on the corrosion phenomena and its complete coverage of the surface of specimens under irradiation. Potentiodynamic polarization proved that the very best value of inhibition efficiency is 95.3% obtained by

50 ppm AO after being irradiated with γ-rays at 298 K. The η% values are in good agreement with those obtained from the EIS measurements.

References

B. Ramesh Babu and K. Thangavel, The effect of isomers of some organic compounds as inhibitors for the corrosion of carbon steel in sulfuric acid, Anticorros Methods Mater, 52 (2005), 219–225.

A. S. Fouda, H. A. Mostafa, F. El-Taib, and G. Y. Elewady, Synergistic influence of iodide ions on the inhibition of corrosion of C-steel in sulphuric acid by some aliphatic amines, Corros Sci, 47 (2005), 1988–2004.

S. Zhang, Z. Tao, W. Li, and B. Hou, The effect of some triazole derivatives as inhibitors for the corrosion of mild steel in 1M hydrochloric acid, Appl Surf Sci, 255 (2009), 6757–6763.

R. Javaherdashti, A review of some characteristics of MIC caused by sulfate-reducing bacteria: past, present and future, Anticorros Methods Mater, 46 (1999), 173–180.

R. Javaherdashti, Impact of sulphate-reducing bacteria on the performance of engineering materials, Appl Microbiol Biotechnol, 91 (2011), 1507–1517.

A. Y. Musa, A. Mohamad, A. H. Kadhum, M. S. Takriff, and L. T. Tien, Synergistic effect of potassium iodide with phthalazone on the corrosion inhibition of mild steel in 1.0M HCl, Corros Sci, 53 (2011), 3672–3677.

H. Ashassi-Sorkhabi, D. Seifzadeh, and M. G. Hosseini, EN, EIS and polarization studies to evaluate the inhibition effect of 3H-phenothiazin-3-one, 7-dimethylamin on mild steel corrosion in 1M HCl solution, Corros Sci, 50 (2008), 3363–3370.

A. K. Singh and M. A. Quraishi, Effect of Cefazolin on the corrosion of mild steel in HCl solution, Corros Sci, 52 (2010), 152–160.

P. Lowmunkhong, D. Ungthararak, and P. Sutthivaiyakit, Tryptamine as a corrosion inhibitor of mild steel in hydrochloric acid solution, Corros Sci, 52 (2010), 30–36.

N. Lotfi, H. Lgaz, M. Belkhaouda, M. Larouj, R. Salghi, S. Jodeh, et al., Effect of anise oil as a green inhibitor on steel corrosion behaviour, Arab J Chem Environ Res, 1 (2014), 13–23.

A. Ostovari, S. M. Hoseinieh, M. Peikari, S. R. Shadizadeh, and S. J. Hashemi, Corrosion inhibition of mild steel in 1M HCl solution by henna extract: A comparative study of the inhibition by henna and its constituents (Lawsone, Gallic acid, a-d-Glucose and Tannic acid), Corros Sci, 51 (2009), 1935–1949.

T. Ibrahim, H. Alayan, and Y. Al Mowaqet, The effect of Thyme leaves extract on corrosion of mild steel in HCl, Prog Org Coat, 75 (2012), 456–462.

D. B. Hmamou, R. Salghi, A. Zarrouk, O. Benali, F. Fadel, H. Zarrok, et al., Carob seed oil: an efficient inhibitor of C38 steel corrosion in hydrochloric acid, Int J Ind Chem, 3 (2012), 25.

L. Afia, R. Salghi, E. Bazzi, L. Bazzi, M. Errami, O. Jbara, et al., Testing natural compounds: Argania spinosa kernels extract and cosmetic oil as ecofriendly inhibitors for steel corrosion in 1M HCl, Int J Electrochem Sci, 6 (2011), 5918–5939.

N. Lahhit, A. Bouyanzer, J. M. Desjobert, B. Hammouti, R. Salghi, J. Costa, et al., Fennel (Foeniculum vulgare) essential oil as green corrosion inhibitor of carbon steel in hydrochloric acid solution, Port Electrochim Acta, 29 (2011), 127–138.

M. H. Hussin and M. J. Kassim, The corrosion inhibition and adsorption behavior of Uncaria gambir extract on mild steel in 1M HCl, Mater Chem Phys, 125 (2011), 461–468.

X. Li and S. Deng, Inhibition effect of Dendrocalamus brandisii leaves extract on aluminum in HCl, H_3PO_4 solutions, Corros Sci, 65 (2012), 299–308.

C. R. R. Araújo, G. M. Corrêa, V. G. da Costa Abreu, T. de Melo Silva, A. M. B. Osorio, P.M. de Oliveira, et al., Effects of gamma radiation on essential oils: A review, in New Insights on Gamma Rays, A. M. Maghraby, ed., IntechOpen, London, 2017, 179–201.

S.-L. Shim, I.-M. Hwang, K.-Y. Ryu, M.-S. Jung, H.-y. Seo, H.-Y. Kim, et al., Effect of γ-irradiation on the volatile compounds of medicinal herb, Paeoniae Radix, Radiat Phys Chem, 78 (2009), 665–669.

M. Müller and G. Buchbauer, Essential oil components as pheromones. A review, Flavour Fragr J, 26 (2011), 357–377.

A. A. El-Meligi and N. Ismail, Hydrogen evolution reaction of low carbon steel electrode in hydrochloric acid as a source for hydrogen production, Int J Hydrogen Energy, 34 (2009), 91–97.

R. S. Farag and K. H. El-Khawas, Influence of γ-irradiation and microwaves on the antioxidant property of some essential oils, Int J Food Sci Nutr, 49 (1998), 109–115.